J Mater Sci (2010) 45:1354–1360
DOI 10.1007/s10853-009-4091-6

High strength bio-composite films of poly(vinyl alcohol) reinforced with chemically modified-fly ash

Dilip Chandra Deb Nath · Sri Bandyopadhyay · Aibing Yu · Darryl Blackburn · Chris White

Received: 1 September 2009 / Accepted: 25 November 2009 / Published online: 9 December 2009

Abstract Fly ash (FA) was chemically modified by activation with sodium hydroxide and used in fabrication of bio-composite films with poly(vinyl alcohol) (PVA) by aqueous casting method. The particle size distribution patterns of modified-fly ash (MFA) were shifted from 2–20 μm to the higher regions 2–40 μm in the analysis chart of Malvern Light Scattering Particle Size Analyser (MLSPSA). On the oxides based chemical analysis by X-ray Fluorescence Spectroscopy (XRF), the compositions of major oxides, SiO_2 73.5%, Al_2O_3 19.2% and Na_2O 1.4% were significantly changed to SiO_2 52.9%, Al_2O_3 23.6% and Na_2O 5.9%, due to the dissolution and re-crystallisation of new phases which are characterised by X-ray diffraction (XRD). The composite film reinforced with 20 wt% MFA showed up to higher tensile strength 289% (three-fold) compared to those of unmodified FA filled films. The alkali treatment (sodium hydroxide) of FA is a very promising approach to improve the mechanical strength, and hence, further enhance the potential for recycling FA as a suitable filler material in bio-composite materials.

Introduction

The polymer composite materials show higher modulus, strength, heat resistance, lower the gas permeability and flammability than neat polymer [1]. The mechanical properties of composites generally depend on the filler's chemical nature, size distribution, aspect ratio, volume fraction, and the intrinsic adhesion between the surfaces of filler and polymer [2]. High aspect ratio of filler increases the yield strength due to the flexibility in adjusting high local stress induced from the polymer matrix [3]. The formation and development of stronger interfacial interaction is critical for the rigidity of composite materials. Therefore, the polymers having the choice of functional groups are desired for the fabrication of high strength composite materials. Polyvinyl alcohol (PVA) is one of the promising biodegradable and water-soluble polymer which is used in the fabrication of environmentally compatible composites with a range of fillers such as, sugar cane [4], starch [5], clay [6], carbon nanotube [7], wood dust [8], cement [9], organo-ceramic [10], and TiO_2 [11]. PVA and its composites are potentially applied in a variety of industrial application, for example, in fibre and textiles industries for sizing and finishing, coating, adhesives, emulsifiers, colloidal stabilisers, and film packaging in food and optical holographic industries [12].

The most electricity in the world comes from pulverised coal-fired boiler in which fly ash is the predominant combustion solid residue. Fly ash is a fine-grained, powdery material that is carried off in the flue gas and usually collected by means of electrostatic precipitators, baghouses, or cyclones. The storage and handling of fly ash are challenging tasks in the context of environmental impact. Some of fly ash is used in landfill, but a large volume still remains unused and needs other sound environmental solutions to dispose and recycle [13].

Due to variations of coal properties, the fly ash properties can vary and often divided into two classes mainly on the basis of calcium levels. Generally high rank coals such

D. C. D. Nath · S. Bandyopadhyay (✉) · A. Yu
School of Material Science and Engineering, The University of New South Wales, Sydney, NSW, Australia
e-mail: S.Bandyopadhyay@unsw.edu.au

D. Blackburn · C. White
Research and Ash Development, Cement Australia, Brisbane, QLD, Australia

as anthracite or bituminous provide Class F ash while lower rank coals provide Class C type ash. Fly ash contains a range of alkali and transition metal elements which are commonly represented as oxides of Si, Al, Fe, Ca, Mg, K and Na even though these occur as complex mineral and glassy phases [14]. Fly ash is well known to show pozzolanic properties due to the presence of glassy aluminosilicate which in the presence of water reacts with lime to produce cementitious product. In addition to pozzolanic properties, Class C fly ash also exhibits self-cementing properties.

Use of FA as filler has been studied to design composite materials with metal matrix [15] as well as polymer matrix including polyester [16], epoxy [17], polypropylene (PP) [18–20], and PVA [21]. In case of the PP composite, the spherical FA is reported to dramatically decrease the tensile strength at room temperature test [20].

Recently, FA has been treated by alkali hydroxides, sodium silicate and aluminate before using to improve cement properties [22–26]. FA activation has been reported to significantly improve early hardening time as well as the mechanical strength of the cement [22]. During activation, Si–O–Si and Al–O–Al bonds of major FA constituents such as aluminosilicate, quartz and mullite are broken to form new bonds which modify their crystal structure [25]. These new modified structure of fly ash alumina-silicates are often identified as the compounds of zeolite precursor family, e.g. faujasite, phillipsite and hydroxysodalite [26, 27]. The nature and amount of activating agents, treatment time and temperature, FA chemistry and the concentration of –OH ions have critical impact in controlling the mechanical properties of cementations materials [25].

In our recent study, we reinforced FA with PVA to increase the mechanical strength of bio-composite [21]. In continuation of that study, we attempted to further enhance and control the mechanical strength of the composite films using chemical activation of Class F type ash. In the present study, FA was treated with alkali in order investigate the chemically modification as a potential quantitative strength parameter. The primary aim of this study is to report the effect of alkali treatment on the modification of the chemical characteristics of fly ash and the implication of using the modified fly ash as filler on the improvement of mechanical strength of PVA composite films.

Experimental procedure

Materials

FA sample was obtained from Swanbank Coal Fire Plant, Cement Australia, Queensland. On the basis of low calcium composition, this fly ash may be considered as Class F fly ash. Poly(vinyl alcohol) (PVA) (Mw: 125,000 and degree of hydrolysis approx. 89%) was purchased from Fine-Chemical Ltd, Chennai, India. Glutaraldehyde (GLA) (25% contents in water) and reagent grade sodium hydroxide (NaOH) were purchased from Laboratory Unilab Reagent and used as received.

Preparation of modified-fly ash (MFA)

Two molar NaOH deionised water solution was prepared. After cooling down the solution, 100 mL was taken in two-necked round bottom flask with attached condenser and placed in oil bath under magnetic stirrer followed by mixing 15 g of FA particles and sealing. The suspension was heated under vigorous stirring at 85 °C for 8 h. The cooled suspension was filtered and washed several time with deionised water. Finally MFA was dried under vacuum for 2 days at 50 °C [22–27]. The higher concentrations of NaOH (8–12 M at pH $>$ 12) and ratio of fly ash/NaOH = 1/1.2 were reported for activation of fly ash [28, 29].

Fabrication of composite films

The composite films were fabricated by casting method from aqueous solution of PVA and FA/MFA. The neat PVA was dissolved in deionised water at 80 °C to prepare the 1.2 wt% solution. The FA/MFA particles with 5, 10, 15, 20 and 25 wt% concentrations were dispersed and sonicated for 5 min (Ultrasonic cleaner FXPQM; frequency, 50 MHz). For the preparation of cross-linked composite films, 1 N HCl (50 μmL) and 1 wt% GLA solution (0.50 mL) in deionised water were added sequentially to PVA-FA and PVA-MFA solutions. The resulting solution was casted in glass petri dishes and the bubbles were removed by shaking. The casted petri dishes were kept at room temperature until dried. The films were peeled out and dried in oven at 60 °C under vacuum for 6 h. The thickness of the films was 0.05–0.07 mm. The thickness of the films was controlled by using the same amount of total materials and same sized 10 cm diameter glass petri dish [7, 8, 21].

Analytical instruments for characterization

- Malvern Light Scattering Particle Size Analyser (MLSPSA) was used to determine the particle size distribution. The Fly ash samples were suspended into the sample cell with aqueous solution after agitating in an ultrasonic bath to obtain maximum dispersion of particles.
- The chemical composition of FA and MFA was obtained using X-ray Fluorescence Spectroscopy (XRF, PanAlytical PW 2400 with Rh end-window tube) method. The samples were prepared as 40 mm

glass beads using lithium meta-borate as a fluxing agent. The XRF is calibrated for a wide range of elements using certified reference materials prepared as glass beads for major element oxides, using optimum machine parameters, and correcting for spectral overlapping lines. Software used was "Super Q" and all majors are expressed as oxides.

- Wide angle X-ray diffraction (WAXRD) spectra of Fly ash samples were obtained using Philips Multipurpose diffractometer (MPD-Scherrer). The spectra were collected over a 2θ range from 5° to 90° with a step size 0.02 and 0.5 s at each step using diffracted beam graphite monochromators with Ni filtered CuKα radiation source generated at 40 kV and 20 mA. The X-pert Software was used to identify minerals [13].
- Hitachi 4500-II scanning electron microscope was used to examine the morphology of ash particles at accelerating voltages 20 kv and working distance $Z = 15$. All specimens were coated with chromium using two sputtering cycles to improve the conductivity of surfaces and hence image quality.
- Philips CM200 TEM (Transmission Electron Microscopy) was used with a field emission gun, which provides very high resolution. The ash particles were dispersed in ethanol followed by sonication. A drop of diluted suspension was poured onto copper grid, which was directly injected in the sample injection holder after air drying.
- XPS (X-ray Photoelectron Spectroscopy) experiment was undertaken for determination of hydroxyl concentration on FA and MFA surfaces under high vacuum generator instrument model Escalb 220-IXL with resolution of 0.8 eV at 240 W (Al K α, 12 kV).
- FA and MFA were characterised by FTIR spectroscope (NEXUS-870, Thermo Nicolet Corporation) running with Omnic software. The condition for the measurement of FTIR: detector, MCT/A; base splitter, KBr; window, diamond; velocity, 0.6329; aperture, 100; scan, 64.
- The tensile yield strengths of the composite samples were determined using an Instron 1185 with crosshead movement 50 mm/min. The specimens were prepared as ASTM D882-95a (length 22 mm, width 5 mm and thickness 0.05 mm) [6, 8, 21]. Five samples were tested in each category and the average value is reported in this article.

Results and discussion

FA and MFA size distribution patterns

Figure 1 compares the particle size distribution patterns of fly ashes before and after alkali activation. This figure

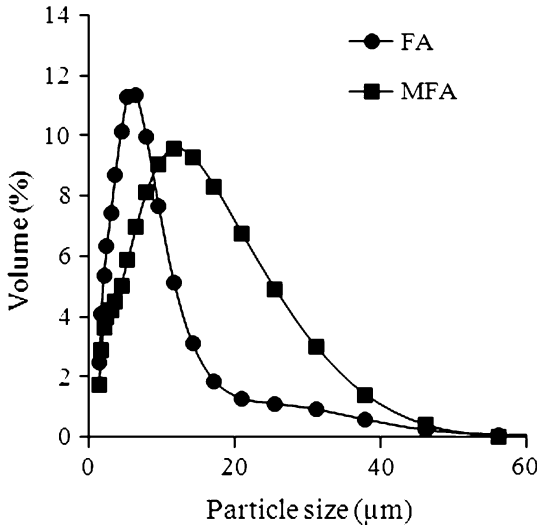

Fig. 1 Particle size distributions of MFA and FA determined by Malvern Light Scattering size Analyser

distinctly shows that before activation, the majority of particles are in a narrow range 0–25 μm while after activation the percentage of particles with larger size range (20–40 μm) increase as indicated by shifting of size distribution curve towards right hand side. The increased size range is believed to occur due to the formation of new crystalline structures, based on similar approach noted synthesis of zeolite [26, 27]. Acid treatment of fly ash particles also showed the increased particle sizes due to existence of the high level agglomeration and/or chemically changed the crystalline structure [30, 31].

Chemical and mineralogical compositions of FA and MFA

The chemical compositions of both fly ash samples are represented as oxide-based analysis by XFS as shown in Table 1. The percentages of major oxides of silicon, aluminium and sodium were changed from 73.5, 19.2 and 1.4 in FA to 52.9, 23.6 and 5.9 in MFA, respectively. The changes occurred due to the formation of structurally new crystalline phases in MFA which is supported from the appearing of new crystalline peaks in MFA in XRD spectrum as shown with FA in Fig. 2. In the XRD spectrum of MFA, there are several new peaks at 12.4, 17.6, 21.6 and 28.2 (2θ°) appeared. Several new peaks appeared are belonged to the combination of zeolite family [22, 28]. The selected peaks along the *d*-spacing were presented to compare the degree of shifting in Table 2.

XRD spectrum of FA distinctly shows quartz (hexagonal, SiO_2) and mullite (orthorhombic, $3Al_2O_3$, $2SiO_2$) peaks while hematite (Fe_2O_3) and magnetite (Fe_3O_4) peaks were not clearly visible possibly due to trace contents in material. Silicon is found in FA as quartz and glassy

Table 1 Chemical compositions of fly ashes analysed by XRF

Compounds	Unmodified fly ash (FA)	Modified fly ash (MFA)
SiO_2	73.55	52.97
Al_2O_3	19.25	23.66
Fe_2O_3	0.97	0.94
CaO	0.99	1.15
MgO	0.60	0.61
TiO_2	1.31	1.64
BaO	0.08	0.09
Cr_2O_3	0.15	0.16
K_2O	0.29	0.32
MnO	0.01	0.61
Na_2O	1.48	5.93
P_2O_5	0.05	0.01
SrO	0.02	0.03
LOI	0.31	11.64
Total	100	100

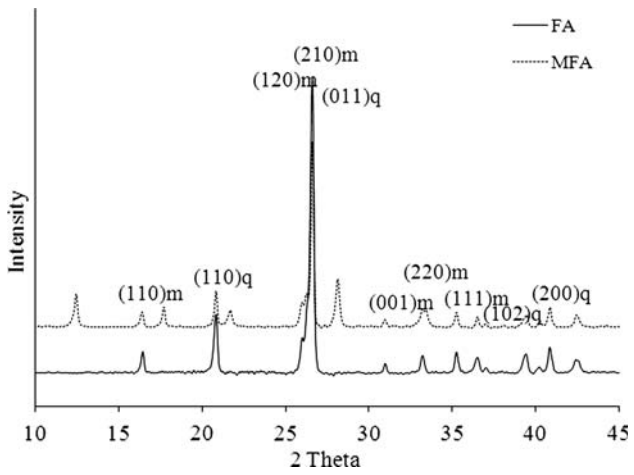

Fig. 2 XRD spectra of MFA and FA

Table 2 The selected peaks of unmodified and modified fly ashes measured by WAXRD

Without modification (FA)		With modification (MFA)	
2θ position (degree)	d-spacing (Å)	2θ position (degree)	d-spacing (Å)
–	–	12.4	7.1
16.4	5.4	16.3	5.4
–	–	17.6	5.0
20.8	5.3	20.8	4.2
–	–	21.6	4.1
25.9	3.4	25.9	3.4
26.2	3.4	26.2	3.4
–	–	28.1	3.2

aluminosilicate, and formed due to decomposition and reaction of quartz, clays and pyrite in parent coal. The major percentage of FA mullite is not an ingredient of the sources of FA coal. The formation of mullite is occurred in the process of thermal decomposition of natural mineral kaolinite in coal combustion process [9], whereas the chemical reactions and thermodynamic studies of activation fly ash with sodium hydroxide were also reported [32, 33].

FA and MFA morphologies

Effect of alkali activation on the morphology of the fly ash particles can be seen from the visual analysis of SEM and TEM images. Figure 3a and b provides SEM images of typical fly ash particles before and after alkali activation. Comparison morphology of fly ash particles in two images clearly shows the distinction of particle sizes and their shapes. In FA sample, the smaller fly ash particles look spherical and smooth-surfaced while relatively larger particles shows highly irregular exterior surface and appear non-spherical like hexagonal in shape (Fig. 3a). Further examinations of the non-spherical bigger particles show the presence of much finer particles on their crystalline surfaces. Figure 3b illustrates that unlike original fly ash sample small sized smooth spherical particles have significantly decreased or disappeared while the percentage of relatively larger size ash particles have increased. This observation is consistent with size analysis data seen in Fig. 1.

The morphology of MFA particles in Fig. 3b further suggests that the increasing number of large sized particles have stacked together to form relatively larger irregular aggregate of multiple stacks of particle which resembles tetragonal in shape. The activation process decreases the proportions of smaller spherical particles while the proportions of relatively larger multilayer irregular aggregates increase. Multiple stacked layers are known to have high aspect ratios and have weak inter-particle forces, which is a potential factor for increasing the interfacial bonding with polymer in composite fabrication [26].

Figure 4a and b shows TEM images of fly ash particles to further illustrate the changes in morphology and surface features of particles. The existences of interfacial interactions among ash particles are distinctively clear with visible clouds in Fig. 4a. This particle–particle interfacial interaction completely disappeared with narrower crystalline shape like needle as seen in MFA particles in Fig. 4b.

Consequently, the agglomeration tendencies of modified ash particles were decreased. This means that the intimate contact areas of MFA particles with polymer matrix will be higher compared to FA particles. This would contribute to better interfacial interaction of polymer matrix and fly ash

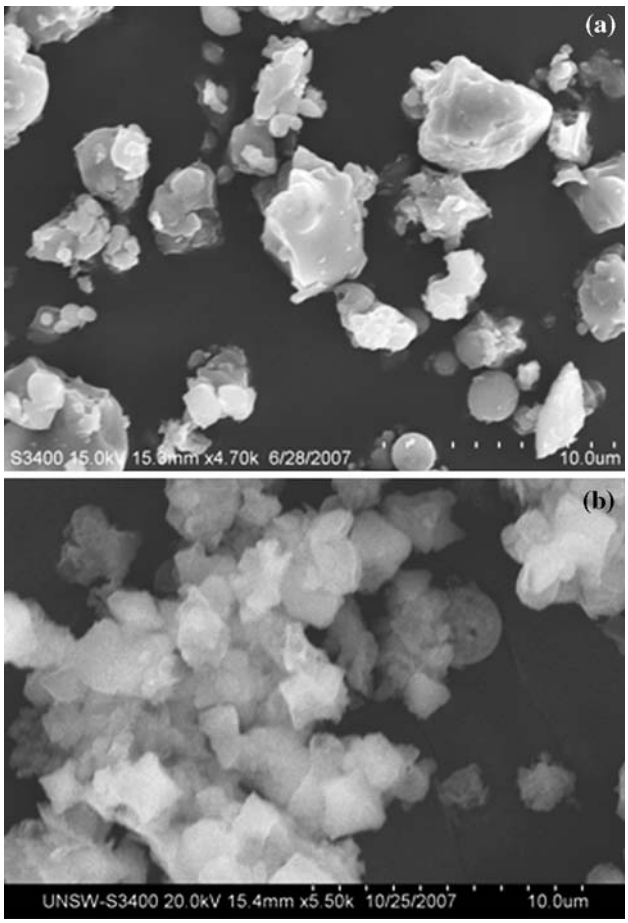

Fig. 3 SEM morphology images of fly ashes, **a** FA and **b** MFA

filler would have critical impact on mechanical strength and fabrication of composite films as higher level of interfacial interaction leads to higher mechanical strength of composite materials [4, 21].

FA and MFA surface topographies

A common functional hydroxyl (–OH) group or ion in general covers the surfaces of metal and metalloid oxides under an atmospheric condition, which has significant role in the formation of physical bonding to the surfaces of substrates. The presence of –OH in fully hydroxyl silica powder has been identified elsewhere [34, 35]. As the major ingredients of FA are mullite and α-quartz which are structured by the oxides of silicon, aluminium, therefore we have made an attempt to examine the level of –OH group presence on FA surface by XPS method, as shown in Fig. 5. The binding energy 95–110 eV of silica and mullite is shown. The peak clearly combined of –OH and –O– attached to α-quartz SiO_2 and mullite are present at the binding energy 103.7 eV. The –OH group on the surface of FA is considered in the formation of interfacial interactions

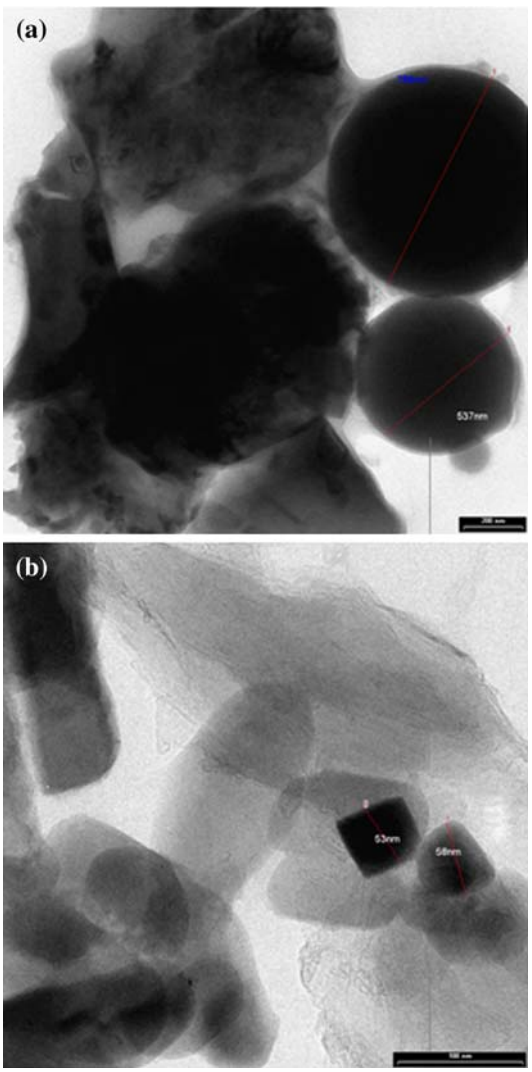

Fig. 4 TEM morphology images of fly ashes, **a** FA and **b** MFA

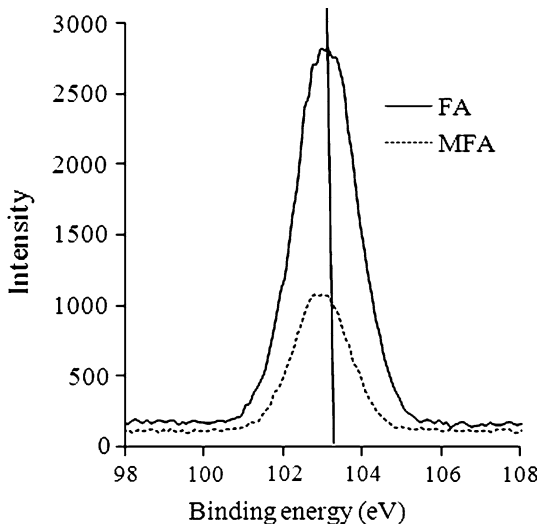

Fig. 5 XPS spectra of FA and MFA

with PVA chain by hydrogen bonding reported recently [35]. The binding energy peak of MFA was shifted by 2 eV lower regions than the ranges of 95–110 eV in FA. Shifting of photoelectron peaks to higher binding energies and the major silicate band to higher energy field has been attributed to the polymerization of the silicate for cements and other clay-like materials [31].

Structural configuration of FA and MFA

FTIR spectra of fly ash samples are shown in Fig. 6 while the selected band positions are summarised in Table 3. FTIR spectrum of FA shows four characteristics stretching vibration bands at 1065 and 798, 779 and 698 cm^{-1}. The stretching vibrations of Si–O–Al bonds occur mainly from 1,200 to 600 cm^{-1}. The strong and broad band at 1,065 cm^{-1} can be related to v3 (Si–O and Si–O–Al) asymmetric stretching vibration while 798 cm^{-1} band can be related to v4 (Si–O–Si) symmetric vibration [28] as well as AlO_4 vibrations [25, 36, 37]. In MFA spectrum, the main band of Si–O– and Al–O– vibrations has clearly shifted towards higher wave number at 1,011 cm^{-1}. Other band peaks also shifted to higher wave number. Therefore, the XPS result clearly supports that alkali treatment contributes to the rearrangement of bonding between the Al–O/Si–O with NaOH.

Mechanical properties of composite films

The relationships of tensile strength with strain of neat PVA and composite films reinforced with 20 wt% FA and MFA are shown in Fig. 7. The tensile strength of the composite films was found to increase in proportional with the addition of fly ashes up to 20 wt% and achieved the maximum 49 and 414% higher strength by FA and MFA than that of neat PVA, respectively. The tensile strength of composite film with MFA particles is about four-fold (289%) higher compared to that of composite film with FA.

The strain at break shows the reverse order of tensile strength phenomena with the addition of FA/MFA and the strains at failures dramatically decreased with due to the formation of stronger interfacial interaction in the ternary component systems, PVA, MFA and GLA.

The strong interfacial interactions restrict the mobility of molecular chain of PVA. The spherical fly ash particles decreased the tensile strength of PP composite at room temperature test [20]. The non-polar PP has less chance to form an interfacial interaction zone to the fly ash surface physically and/or chemically. The formation of interfacial interaction between two small different molecules in polymer composite play a significant role in the improvement of mechanical strength compared to neat polymer [21].

PVA is a hydrophilic polymer matrix, which shows the formation of intra and inter molecular hydrogen bonding between the –OH and $–COOCH_3$ groups presence in the partial-hydrolysed PVA molecular chains [12]. The –OH

Table 3 The selected FTIR absorption peaks of FA and MFA

Samples	Stretching vibrations peaks of structural groups at (cm^{-1})			
	Si–O/Al–O	Al–O	Al–O	Al–O
FA (without modification)	1065	796	779	698
MFA (with modification by NaOH)	1011	802	783	698

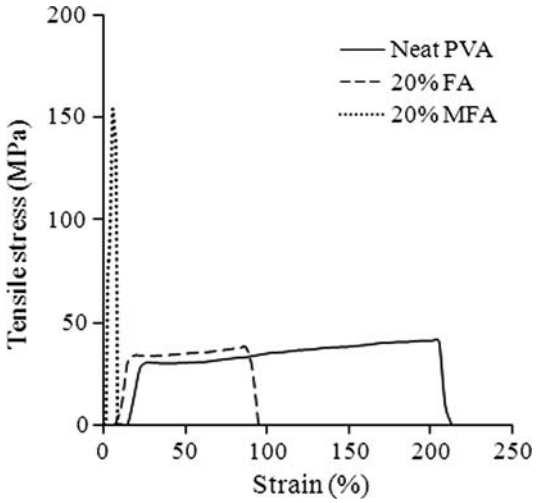

Fig. 7 Relationship of tensile stress and strain of neat PVA and the composite films reinforced with 20 wt% MFA and FA

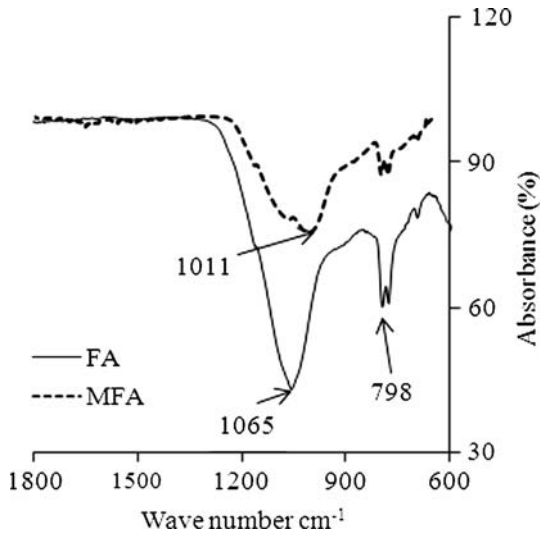

Fig. 6 FTIR spectra of FA and MFA

groups on the surface of fly ash particle may participate in the formation of hydrogen bonds with PVA and chemically cross-linked with GLA molecules. The degree of bonding certainly determined the strength of the composite films. The details of cross-linking mechanisms were recently reported with plausible physical models in the binary system PVA and FA [21], and in the ternary systems PVA, FA and GLA [38].

Conclusions

The following conclusions were made based on the fabrication study of bio-composite films of PVA reinforced with modified and unmodified fly ashes.

- The study shows that after NaOH treatment, the size distribution of fly ash sample is changed such that the percentage of coarser size fraction (20–40 μm) increases.
- The percentage of most oxides of elements, Si, Al and Na decreased which can be attributed to the dissolution and recrystallisation of new phases. The activation process changed the spherical morphology of FA particles to narrower needle-like shape in MFA.
- The particle–particle interaction forces in FA were removed by the activation process which play significant role in enhancement of mechanical strength in composite films
- The tensile strength of composite film with MFA particles is about four-fold (289%) higher compared to that of composite film with FA.
- With improved understanding of alkali treatment of fly ash, there is great potential for recycling fly ash as a suitable filler material in bio-composite materials.

References

1. Ray SS, Okamoto M (2003) Prog Polym Sci 28:1539
2. Tjong SC, Li RKY, Cheung T (1997) Polym Eng and Sci 37(1):166
3. Bigg DM (1987) Polym Compos 8(2):115
4. Chiellini E, Cinelli P, Imam SH, Mao I (2001) Biomacromolecules 2:1029
5. Ramaraj B (2007) J Appl Polym Sci 103:909
6. Strawhecker KE, Manias E (2000) Chem Mater 12:2943
7. Zhang X, Liu T, Sreekumar TV, Kumar S, Moore VC, Hauge RH, Smalley R (2003) Nano Lett 3(9):1285
8. Bana R, Banthia AK (2007) Polym-Plast Tech Eng 46:821
9. Weichold O, Moller M (2007) Adv Eng Mater 9(8):712
10. Tan LS, Mchugh AJ (1996) J Mater Sci 31:3701. doi: 10.1007/BF00352783
11. Chen X (2002) J Mater Sci Lett 21:1637
12. Huang H, Gu L, Ozaki Y (2006) Polymer 47:3935
13. Ward CR, French D (2006) Fuel 85:2268
14. Alkan C, Arslan M, Cici M, Kaya M, Aksoy M (1995) Resour Conserv Recyl 13:147
15. Kojima Y, Usuki A, Kawasumi M, Fukushima Y, Okada A, Kurauchi T, Kamigaito O (1993) J Mater Res 8:1179
16. Guhanathan S, Sarojadevi M (2004) Comp Interface 11(1):43
17. Gupta N, Brar BS, Woldesenbet E (2001) Bull Mater Sci 24(2):219
18. Nath DCD, Bandyopadhyay S, Yu A, Blackburn D, White C (2010) J Appl Poly Sci 115:1510
19. Nath DCD, Bandyopadhyay S, Yu A, Blackburn D, White C, Varughese S (2009) J Therm Anal Calorim (in press). doi: 10.1007/s10973-009-0408-6
20. Nath DCD, Bandyopadhyay S, Yu A, Zeng Q, Das T, Blackburn D, White C (2009) J Mater Sci 44:6078. doi:10.1007/s10853-009-3839-3
21. Nath DCD, Bandyopadhyay S, Boughton P, Yu A, Blackburn D, White C (2009) J Appl Poly Sci (in press)
22. Fan Y, Yin S, Wen Z, Zhong J (1999) Cement Concrete Res 29:467
23. Xie Z, Xi Y (2001) Cement Concrete Res 31:1245
24. Shi C, Day RL (1995) Cement Concrete Res 25(1):15
25. Palomo A, Grutzeck MW, Blanco MT (1999) Cement Concrete Res 29:1323
26. Tanaka H, Furusawa S, Hino R (2002) J Mater Syn Process 10(3):43
27. Palomo A, Blanco MT, Granizo ML, Puertas F, Vazquez T, Grutzeck MW (1999) Cement Concrete Res 29:997
28. Chang HL, Shih WH (1998) Ind Eng Chem Res 37:71
29. Jimenez AF, Palomo A (2005) Cement Concrete Res 35:1984
30. Roode MV, Douglas E, Hemmings RT (1987) Cement Concrete Res 17:183
31. Mollah MYA, Hess TR, Cocke D (1994) Cement Concrete Res 24:109
32. Jimenez AF, Palomo A (2003) Fuel 82:2259
33. Brouwers HJH, Eijk RJV (2003) In: Proceedings of the 11th international congress on the chemistry of cement (ICCC) 11–16 May, Durban, South Africa, Cements contribution to the development in the 21st century. ISBN Number: 0-9584085-8-0
34. Mueller R, Kammler HK, Wegner K, Pratsinis SE (2003) Langmuir 19:160
35. Paparazzo E (1996) Surf Inter Anal 24:729
36. Nath DCD, Bandyopadhyay S, Gupta S, Yu A, Blackburn D, White C (2009) App Surf Sci. doi:10.1016/j.apsusc.2009.11.024
37. Kaczmarek H, Podgorski A (2007) J Photochem Photobiol A 191:209
38. Nath DCD, Bandyopadhyay S, Yu A, Blackburn D, White C (2009) J Appl Poly Sci (under review)